Published in final edited form as:
Arterioscler Thromb Vasc Biol. 2013 November ; 33(11): 2549–2557. doi:10.1161/ATVBAHA.113.301588.

Capillary Endothelial Fatty Acid Binding Proteins 4 and 5 Play a Critical Role in Fatty Acid Uptake in Heart and Skeletal Muscle

Tatsuya Iso[*], **Kazuhisa Maeda**[*], **Hirofumi Hanaoka**, **Toshihiro Suga**, **Kosaku Goto**, **Mas Rizky A.A Syamsunarno**, **Takako Hishiki**, **Yoshiko Nagahata**, **Hiroki Matsui**, **Masashi Arai**, **Aiko Yamaguchi**, **Nada A. Abumrad**, **Motoaki Sano**, **Makoto Suematsu**, **Keigo Endo**, **Gökhan S. Hotamisligil**, and **Masahiko Kurabayashi**
Department of Medicine and Biological Science (T.I., T.S., K.G., M.R.A.AS., H.M., M.A., M.K.), Education and Research Support Center (T.I., M.K.), Department of Bioimaging Information Analysis (H.H., A.Y.), and Department of Diagnostic Radiology and Nuclear Medicine (K.E.), Gunma University Graduate School of Medicine, Maebashi, Gunma, Japan; Department of Genetics and Complex Diseases and Nutrition, Broad Institute of Harvard and MIT, Harvard School of Public Health, Boston, MA (K.M., G.S.H.); Department of Biochemistry (T.H., Y.N., M.S.), JST, ERATO, Suematsu Gas Biology Project (T.H., Y.N., M.S.), and Department of Cardiology (M.S.), Keio University School of Medicine, Tokyo, Japan; and Department of Medicine, Center for Human Nutrition, Washington University School of Medicine, St. Louis, MO (N.A.A.)

Abstract

Objective—Fatty acids (FAs) are the major substrate for energy production in the heart. Here, we hypothesize that capillary endothelial fatty acid binding protein 4 (FABP4) and FABP5 play an important role in providing sufficient FAs to the myocardium.

Approach and Results—Both FABP4/5 were abundantly expressed in capillary endothelium in the heart and skeletal muscle. The uptake of a FA analogue, 125I-15-(*p*-iodophenyl)-3-(R,S)-methyl pentadecanoic acid, was significantly reduced in these tissues in double-knockout (DKO) mice for FABP4/5 compared with wild-type mice. In contrast, the uptake of a glucose analogue, 18F-fluorodeoxyglucose, was remarkably increased in DKO mice. The expression of transcripts for the oxidative catabolism of FAs was reduced during fasting, whereas transcripts for the glycolytic pathway were not altered in DKO hearts. Notably, metabolome analysis revealed that phosphocreatine and ADP levels were significantly lower in DKO hearts, whereas ATP content was kept at a normal level. The protein expression levels of the glucose transporter Glut4 and the phosphorylated form of phosphofructokinase-2 were increased in DKO hearts, whereas the phosphorylation of insulin receptor-β and Akt was comparable between wild-type and DKO hearts during fasting, suggesting that a dramatic increase in glucose usage during fasting is insulin

Correspondence to Tatsuya Iso, MD, PhD, Department of Medicine and Biological Science, Gunma University Graduate School of Medicine, 3-39-22 Showa-machi, Maebashi, Gunma 371-8511, Japan. isot@gunma-u.ac.jp.
[*]These authors contributed equally to this article.
Current address for K.M.: Department of Complementary and Alternative Medicine, Graduate School of Medicine, Osaka University Hospital, Osaka, Japan.
Current address for H.H.: Department of Molecular Imaging and Radiotherapy, Graduate School of Pharmaceutical Sciences, Chiba University, Chiba, Japan.

Disclosures
None.

The online-only Data Supplement is available with this article at http://atvb.ahajournals.org/lookup/suppl/doi:10.1161/ATVBAHA.113.301588/-/DC1.

independent and is at least partly attributed to the post-transcriptional and allosteric regulation of key proteins that regulate glucose uptake and glycolysis.

Conclusions—Capillary endothelial FABP4/5 are required for FA transport into FA-consuming tissues that include the heart. These findings identify FABP4/5 as promising targets for controlling the metabolism of energy substrates in FA-consuming organs that have muscle-type continuous capillary.

Keywords

capillaries; endothelial cells; fatty acid binding proteins; fatty acids; glucose; metabolism

---

The heart requires a tremendous amount of ATP as the primary energy source to maintain efficient contractile function. Because the myocardial ATP pool is limited, the heart needs to constantly generate ATP in response to energy demands by the aerobic oxidation of energy substrates that are primarily nonesterified fatty acids (NEFAs; ≈70%), with glucose and lactate contributing to the rest. Among the many complicated machineries that regulate cardiac energy metabolism, the substrate uptake from circulation and its further transfer to cardiac myocytes through the capillary endothelial cells (ECs) are the first critical components. Because of their low aqueous solubility, FAs are supplied to tissues as albumin-bound complexes or triacylglycerols (TGs) of circulating lipoproteins. In contrast to sinusoidal ECs that have large fenestrates (100–200 nm), which allow for the passage of small particles that include albumin (5–10 nm) and chylomicron remnants (30–80 nm), capillary ECs in the heart and skeletal muscle do not allow these processes. Instead, theoretically, transendothelial FA transport (Figure VI in the online-only Data Supplement), which involves proteins with a high affinity for FAs in the capillary endothelial cytoplasm, would be most likely to supply FAs to cardiac myocytes.[1,2]

Recently, several reports have supported this concept. Hagberg et al[3] showed that vascular endothelial growth factor (VEGF)-B controls the endothelial transport of FAs via the transcriptional induction of the FA transport proteins (FATPs), FATP3 and FATP4, in an endothelial-specific manner. Interestingly, 2 hours after oral gavage, the uptake of ^{14}C-oleic acid was reduced in the heart, muscle, and brown adipose tissue, but not in other tissues in mice that were deficient for VEGF-B, suggesting the tissue-specific regulation of FATP3/4 in vascular response to VEGF-B. It has also been reported that endothelial peroxisome proliferator–activated receptor γ (PPARγ) plays a role in transendothelial FA transport via the induction of its target genes that include fatty acid binding protein 4 (FABP4).[4,5] However, it remains largely unknown to what extent and in what tissues these proteins contribute to overall transendothelial FA transport.

Cytoplasmic FABPs are a family of 14- to 15-kDa proteins that bind with high affinity to hydrophobic molecules, such as long-chain FAs and eicosanoids.[6] As lipid chaperones, FABPs may actively facilitate the transport of lipids to specific compartments in the cells. FABP4 (also known as aP2/ ALBP/A-FABP) and FABP5 (also called mal1/E-FABP) play important roles in the pathogenesis of chronic metabolic diseases through their expression in adipocytes and macrophages. Whereas mice that were singly deficient for FABP4 or FABP5 showed a modest phenotype because of their redundant function,[7–9] mice that lacked both *Fabp4* and *Fabp5* (*Fabp4/5* double-knockout [DKO] mice) displayed a dramatic phenotype in their metabolism or a strong protection against diet-induced obesity, insulin resistance, type 2 diabetes mellitus, atherosclerosis, and fatty liver disease.[10,11] Recently, immunohistochemical analyses revealed that both FABP4/5 are coexpressed in capillary ECs in various tissues, including the heart, skeletal muscle, and adipose tissue.[12,13] Because capillary ECs are the functional interface between circulation and parenchymal cells, their expression in capillary ECs led us to hypothesize that capillary endothelial FABP4/5 may

play a role in the regulation of FA transport through capillary ECs (namely, transendothelial FA transport; Figure VI in the online-only Data Supplement), which may also influence glucose metabolism.

In the present study, we show that capillary endothelial FABP4/5 are required for FA transport into FA-consuming tissues that include the heart and skeletal muscle. We further address the molecular mechanisms that underlie the compensatory glucose usage against the loss of FABP4/5 function.

Results

Capillary Endothelial–Specific Expression of FABP4 and FABP5 in the Heart and Skeletal Muscle

Our reverse transcription polymerase chain reaction (PCR) revealed that both *Fabp4* and *Fabp5* are expressed in adipose tissue and other tissues that include the heart and skeletal muscle (Figure I in the online-only Data Supplement). As predicted, in mice that are deficient for FABP4 (*Fabp4*$^{-/-}$), FABP5 (*Fabp5*$^{-/-}$), and both (*Fabp4/5* DKO), the expression of *Fabp4* and *Fabp5* was absent in the adipose tissue and heart of *Fabp4*$^{-/-}$ and *Fabp5*$^{-/-}$ mice, respectively (Figure 1A). Notably, the expression of *Fabp5* was enhanced in *Fabp4*$^{-/-}$ mice, whereas *Fabp4* expression was not altered in *Fabp5*$^{-/-}$ mice (Figure 1A). Immunohistochemistry revealed that FABP4 was strongly expressed in ECs of capillaries and in venules of ventricles, atria, and skeletal muscles, but not in arterioles, arteries, and aorta (Figure 1B; Figure IB in the online-only Data Supplement). Likewise, FABP5 was expressed in ECs of capillaries and venules (Figure 1B; Figure IC in the online-only Data Supplement). Consistent with the results of the reverse transcription PCR (Figure 1A), the expression of FABP5 was enhanced in capillary ECs in *Fabp4*$^{-/-}$ mice (Figure 1B; Figure IC in the online-only Data Supplement), whereas the intensity of FABP4 expression was not altered in *Fabp5*$^{-/-}$ mice (Figure 1B; Figure IB in the online-only Data Supplement), suggesting the predominant function of FABP4 compared with FABP5 in capillary ECs. We also confirmed the expression of FABP4/5 in the capillary ECs of brown and white adipose tissue (Figure ID and IF in the online-only Data Supplement). FABP4 was expressed only in platelet/endothelial cell adhesion molecule-positive ECs that were prepared from mouse heart, but not in other cells (Figure IE in the online-only Data Supplement). The strong expression of FABP4/5 was observed in capillary ECs of human heart and adipose tissue as well (Figure IG in the online-only Data Supplement). Developmentally, FABP4 was induced after birth, whereas FABP5 was detected at embryonic day 18 (Figure I–H in the online-only Data Supplement), suggesting that FABP4 expression contributes to a perinatal shift of fuel preference from glucose to FAs. Interestingly, neither FABP4 nor FABP5 was detected in capillary ECs in the liver, brain, and lung (Figure II in the online-only Data Supplement). These findings indicate that the capillary endothelial expression of FABP4/5 is developmentally regulated in a cell type–specific and tissue-specific manner. Given that the heart and red skeletal muscle are 2 major tissues that consume abundant FAs and must continually generate ATP at a high rate for contraction, sarcoplasmic reticulum Ca^{2+} ATPase, and other ion pumps, their robust expression in capillary ECs led us to investigate the role of FABP4/5 in transendothelial FA transport (Figure VI in the online-only Data Supplement), which is a mechanism recently proposed by several studies.[1–5]

Biodistribution of the FA Analogue 125I-15-(*p*-Iodophenyl)-3-(R,S)-Methyl Pentadecanoic Acid and the Glucose Analogue 18F-Fluorodeoxyglucose in DKO Mice

To directly evaluate the contribution of endothelial FABP4/5 to transendothelial FA transport in vivo, we compared the biodistribution of the slowly oxidized FA analogue 125I-15-(*p*-iodophenyl)-3-(R,S)-methyl pentadecanoic acid (^{125}I-BMIPP) and the

metabolically trapped glucose analogue 18F-fluorodeoxyglucose (^{18}F-FDG). A significant reduction of ^{125}I-BMIPP uptake was observed in the heart, red skeletal muscle, and adipose tissue of *Fabp4/5* DKO mice, but was not observed in either *Fabp4*$^{-/-}$ or *Fabp5*$^{-/-}$ mice (Figure 2A; Figure IIA and IIC in the online-only Data Supplement). Importantly, ^{125}I-BMIPP uptake was not impaired in white skeletal muscles, which use more glucose than FA as an energy substrate. Of particular interest, ^{18}F-FDG uptake increased dramatically in the heart and red skeletal muscle of *Fabp4/5* DKO mice, whereas ^{18}F-FDG uptake did not change in white skeletal muscles, strongly suggesting that an augmentation of glucose uptake occurs to compensate for a reduction in FA uptake in FA-consuming tissues (Figure 2B; Figure IIB and IID in the online-only Data Supplement). A dramatic increase in ^{18}F-FDG uptake was also observed in the hearts of *Fabp4/5* DKO mice by ^{18}F-FDG positron emission tomography imaging (Figure 2C; Figure IIG in the online-only Data Supplement). ^{18}F-FDG uptake was unchanged or slightly decreased in adipose tissues of *Fabp4/5* DKO mice in spite of reduced ^{125}I-BMIPP uptake (Figure 2A and 2B; Figure IIA–IIF in the online-only Data Supplement).

To ensure that FA uptake and glucose uptake were not impaired in cardiac myocytes of DKO mice, we prepared cardiac myocytes from DKO and wild-type (WT) mice and treated them with 14C-palmitic acid and 3H-deoxyglucose. No significant difference was observed in the uptake of either 14C-palmitic acid or ^{3}H-deoxyglucose between DKO- and WT-derived cardiac myocytes (Figure 2D). Taken together, these results suggest that capillary endothelial FABP4/5 significantly contribute to FA uptake in the heart and red skeletal muscle and that the impairment of this pathway induces a compensatory increase in glucose usage.

Changes in the Expression of FA-Handling Genes in the Heart of DKO Mice

We next examined gene expression in hearts with or without a 24-hour fast. The expression levels of several genes that are involved in FA metabolism, including *Fabp3*, FA translocase (FAT/*Cd36*), carnitine palmitoyltransferase 1b (*Cpt1b*), *Cpt2*, acyl-CoA dehydrogenase long chain (*Acadl*), Acad medium chain (*Acadm*), uncoupling protein 2 (*Ucp2*), and *Ucp3*, were lower in DKO mice after a 24-hour fast, whereas the expression levels of these genes were almost comparable between WT and DKO mice during the fed state (Figure 3). The expression of *Ppara* and PPARγ coactivator 1α (*Pgc1a*) between WT and DKO mice was comparable after fasting (data not shown). The level of TGs in the heart tended to increase in WT after fasting; TG levels were markedly lower in DKO than in WT mice (Figure 3B and 3C), which is consistent with reduced uptake of ^{125}I-BMIPP (Figure 2A; Figure IIA and IIC in the online-only Data Supplement). Given that most of the genes in Figure 3 are target genes of PPARα, along with the data that basal expression levels of the genes were comparable during the fed state, it is likely that the downregulation of gene expression in hearts of DKO mice may be a secondary effect of the reduction in endogenous PPARα ligands or long-chain FAs.

Glucose Metabolism and Insulin Signaling in the Heart of DKO Mice

In contrast to the FA-handling genes, a multitude of genes that are involved in glucose metabolism was not significantly affected (Figure III in the online-only Data Supplement). However, the protein expression of Glut4 and the phosphorylation level of phosphofructokinase-2 (PFK2), which is an enzyme that converts fructose-6-phosphate to fructose 2,6-bisphosphate (Fru-2,6-P2, a potent activator for PFK1), increased in *Fabp4/5* DKO hearts in both the fed and the fasted condition (Figure 4A and 4B), which may explain the acceleration of glucose uptake and usage in DKO hearts (Figure VI in the online-only Data Supplement). We further sought to determine whether insulin signal transduction is affected. Insulin signal transduction, which was evaluated by the phosphorylation of insulin

receptor-β and Akt, was equivalent between WT and DKO hearts at the baseline, whereas the insulin-inducible phosphorylation of insulin receptor-β and Akt tended to be increased in DKO mice (Figure 4C and 4D). It should be noted that ^{18}F-FDG uptake was considerably higher in DKO hearts during fasting when insulin signaling was minimized (Figure 2B and 2C; Figures IIB, IID, and VI in the online-only Data Supplement). These findings imply that glucose consumption in the hearts of DKO mice during fasting is promoted independently of the activation of insulin signaling. Together, our data raise the possibility that a dramatic increase in ^{18}F-FDG uptake during fasting could be partially attributed to an increase in Glut4 protein expression and in enhanced phosphorylation of PFK2, which are controlled at the post-transcriptional level independent of insulin signaling (Figure VI in the online-only Data Supplement).

Metabolomic Profiling in Hearts of DKO Mice

We then measured metabolites in hearts. Although ATP levels were comparable, both phosphocreatine (reserve energy) and ADP levels were significantly reduced in DKO hearts (Figure 5A). Given that the ATP concentration in cardiac myocytes should be replenished by phosphocreatine and ADP (Figure 5A), except in end-stage heart failure,[14] the reduction in phosphocreatine and ADP levels strongly suggests that ATP production rate is diminished in the hearts of DKO mice. ATP is also known to act as a potent negative regulator for PFK1 activity in a negative feedback loop in the glycolysis pathway. Therefore, reduced rates of ATP production further promote the glycolysis pathway by activating PFK1 in combination with Fru-2,6-P2, which is produced by phosphorylated PFK2 (Figure 4C; Figure VI in the online-only Data Supplement). Citrate usually becomes *cis*-aconitate in the tricarboxylic acid (TCA) cycle, whereas citrate becomes malonyl-CoA via acetyl-CoA in the FA synthesis pathway during overeating (Figure VI in the online-only Data Supplement). Surprisingly, the level of *cis*-aconitate and its relative ratio to citrate were reduced, whereas the amount of malonyl-CoA relative to citrate significantly increased (Figure 5B), suggesting that a certain amount of citrate is likely to be used in FA synthesis to compensate for the reduced uptake of FAs even during fasting (Figure VI in the online-only Data Supplement). In addition, the concentration of β-hydroxybutyrate, which is a component of ketone bodies, in the heart was 3-fold higher in DKO mice than WT (Figure 5C), suggesting that the ketone body utilization pathway contributes to the source of ATP production in DKO hearts (Figure VI in the online-only Data Supplement). Collectively, our metabolome analysis suggests that the rate of ATP production decreases because of restricted transendothelial FA transport (Figure VI in the online-only Data Supplement). The shortage of FAs is not completely compensated by the significant uptake of glucose because a part of acetyl-CoA, which is derived from glucose, may serve as materials for FA synthesis, leading to an insufficient supply of acetyl-CoA for ATP production (Figure VI in the online-only Data Supplement).

One of the possible mechanisms for increased glycolysis in the energy-deprived heart is thought to be the activation of the AMP-activated protein kinase that senses the energy status of the cells and has a central role in the regulation of major energy-generating metabolic pathways, which include PFK2 phosphorylation.[15,16] In DKO hearts, however, neither the expression nor the phosphorylation of AMP-activated protein kinase was altered compared with WT (Figure 4C and 4D). Consistent with this, the level of AMP and the ratio of AMP/ ATP were comparable between WT and DKO hearts after a 24-hour fast (Figure IV in the online-only Data Supplement), suggesting that AMP-activated protein kinase does not play a significant role in mediating the fasting-induced enhancement of glucose usage in the DKO heart. These findings suggest that additional molecular mechanisms might sense energy depletion.

Mild Cardiac Hypertrophy Similar to Physiological Growth

We then examined the effects of FABP4/5 deficiency on cardiac function as evaluated by heart weight, echocardiography, histology, and myocardial gene expression. Heart weight and heart weight/body weight ratio were significantly higher in DKO mice than WT mice (Table II in the online-only Data Supplement). There were no significant differences in blood pressure, heart rate, ejection fraction, and fractional shortening of left ventricle (Tables II and III in the online-only Data Supplement). Masson Trichrome stain revealed no significant interstitial fibrosis in either DKO or WT hearts (data not shown). The expression of several markers for cardiac overload, such as atrial natriuretic peptide, brain natriuretic peptide, and cardiac myosin heavy chain genes, was comparable between DKO and WT hearts (Figure V in the online-only Data Supplement). These findings indicate that DKO hearts exhibit hypertrophy that is similar to physiological heart growth, which is known to occur during postnatal development or in response to exercise training.

Serum Levels of Lipids, Glucose, and Ketone Bodies

We next examined serum levels of several biochemical parameters before and after a 24-hour fast (Figure 6). The level of glucose was significantly lower in DKO mice than in WT mice after a 24-hour fast, whereas no significant difference in the insulin level was observed. Consistent with reduced uptake of ^{125}I-BMIPP by peripheral tissues during fasting, serum levels of NEFAs increased reciprocally in DKO mice. In parallel with NEFAs, the serum level of ketone bodies was also higher in DKO mice after a 24-hour fast. It is plausible that an increased production of ketone bodies in DKO mice is attributed to elevated levels of serum NEFAs and reduced levels of blood glucose (Figure 2A and 2B; Figure IIA–IIE in the online-only Data Supplement). Ketone bodies are used as alternative energy substrates for peripheral tissues, including hearts in DKO mice, which is consistent with higher concentration of β-hydroxybutyrate in the hearts (Figure 5C). TG levels were lower in DKO during the fed state although TG was comparable during the fasting state (Figure 6). Thus, serum levels of glucose decreased, whereas serum levels of NEFAs and ketone bodies increased, which supports our hypothesis that FA uptake is diminished and a shift of fuel preference toward glucose usage becomes more prominent in the heart and red skeletal muscle in DKO mice during fasting.

Discussion

The present study provides 4 lines of evidence showing that capillary FABP4 and FABP5 play a critical role in the uptake of circulating FAs into the heart and skeletal muscle, a mechanism termed transendothelial FA transport. First, FABP4 in the heart and skeletal muscle was most exclusively expressed in capillary ECs, and the compensatory induction of FAPB5 expression in *Fabp4*$^{-/-}$ mice occurs only in capillary ECs. Second, in *Fabp4/5* DKO mice, FA uptake was markedly reduced, whereas glucose uptake was robustly elevated in the heart and red skeletal muscle, which have high energy demands that are largely met by FA oxidation. Third, cardiac myocytes that were isolated from DKO and WT mice took up ^{14}C-palmitic acid and 3H-deoxyglucose to a similar extent. Last, the difference in glucose uptake between DKO and WT hearts was dramatically enhanced after a 24-hour fast when the serum insulin level was considerably low. Thus, we hypothesize that the dramatic increase in glucose usage in the hearts of fasted DKO mice may not be ascribed to the simple enhancement of insulin sensitivity but rather to the metabolic adaptation that occurred to compensate for reduced FA transport. Collectively, our findings point to the previously underappreciated role of capillary endothelial FABP4/5 in FA transport to cardiac and skeletal myocytes to maintain sufficient ATP production.

Several mechanisms have been proposed to account for the improvement in whole-body inflammatory response and insulin sensitivity in *Fabp4/5* DKO mice. First, FABP4/5 in macrophages and adipocytes contribute to the production of inflammatory cytokines from both cell types, and interactions between these 2 cell types are critical to trigger systemic inflammatory and metabolic responses.[17] Second, an increased supply of adipose tissue palmitoleate (C16:1n7, also termed lipokine)[18] or an increase in the ratio of shorter chain FAs (C14) to longer chain FAs (C18) in adipose and muscle tissues may mediate increased insulin sensitivity and protection from fatty liver.[11] In addition to those mechanisms, our findings that indicated a significant increase in glucose uptake in heart and red skeletal muscle led us to propose that a decrease in endothelial FA transport via FABP4/5 into heart and skeletal muscle may positively contribute to the improved glucose metabolism and insulin sensitivity observed in DKO mice even on a high-fat diet. To verify this hypothesis, we attempted to rescue the defective endothelial FA uptake by generating transgenic mice that express the FABP4 gene under the control of the Tie-2 promoter. Unfortunately, however, the DKO mice carrying Tie-2 promoter-FABP4 seem to be embryonic lethal because few mice were born alive. A few living mice that express FABP4 in ECs in *Fabp4/5* DKO background have a similar phenotype to *Fabp4/5* DKO mice, possibly because expression levels of FABP4 were too low in ECs in those mice to substantially increase FA uptake. Further study should be warranted to understand the role of endothelial FABP4/5 in the regulation of systemic lipid homeostasis and the resulting glucose metabolism.

Earlier studies identified potential regulators for transendothelial FA transport.[3,5] Hagberg et al[3] described the observation that VEGF-B acts on neighboring EC-surface receptors, such as VEGF receptor 1 and neuropilin 1, to stimulate the expression of FATP3/4. Interestingly, although VEGF-B induces a variety of genes that mediate FA handling, including FATPs, VEGF-B does not induce FABP4.[3] In addition, unlike FABP4/5, VEGF-B expression was not induced but rather decreased by fasting. These findings suggest that the mechanisms by which VEGF-B induces FA uptake are distinct from those mechanisms that are induced by FABP4/5. Another evidence supporting the role of the genes coding for FA metabolism in endothelial FA transport was demonstrated using mice deficient in endothelial PPARγ (*Pparg*$^{\Delta EC}$), which impair the expression of PPARγ and its target genes, such as glycosylphosphatidylinositol-anchored high-density lipoprotein-binding protein 1, cellular retinol-binding protein III (also known as RBP7 in mice and RBP5 in humans) and FAT/CD36, as well as FABP4 in an endothelium-specific manner.[5] Our recent study extended those observations by defining the regulation of endothelial FA transport by PPARγ as a response to fasting.[4] In that study, we demonstrated that FA uptake was promoted by PPARγ stimulation via an induction of FABP4 and FAT/CD36 by measuring the uptake of ^{14}C-palmitic acid in cultured capillary EC in the presence or absence of siRNA for FABP4 or FAT/CD36. However, the contribution of each of endothelial PPARγ-target genes to cardiac energetics in vivo remained to be determined. The current study showed that FABP4/5 did play a role in FA uptake in the heart and red skeletal muscle. Studies to test the effects of the endothelial deletion of FAT/CD36 alone or in combination with FABP4/5 on transendothelial FA transport are now in progress.

Mouse models lacking FA-handling genes (eg, PPARα,[19] FAT/CD36,[20] FABP3,[21,22] lipoprotein lipase,[23] and VEGF-B[3]) show that decreased FA oxidation is invariably accompanied by increased glucose oxidation in the heart. However, the mechanisms underlying this observation have yet to be determined. Our present study provides new insight into the mechanism by which the alteration of glucose usage is more obvious in the heart especially during fasting (Figure VI in the online-only Data Supplement). We showed that 18F-FDG uptake was extremely higher in DKO than in WT hearts during fasting when plasma glucose and insulin levels were low, and thus insulin signaling is minimized, implying that accelerated glucose usage during fasting is independent of insulin. In addition,

glucose consumption is enhanced in DKO hearts at multiple steps, which include the post-transcriptional and allosteric regulation of the key proteins that regulate glucose uptake and the glycolysis pathway (ie, an increase in the protein level of Glut4 and the phosphorylation of PFK2). These metabolic shifts toward glucose consumption could be caused by a decrease in the rate of ATP synthesis because of restricted FA uptake. ATP per se also acts as a negative allosteric regulator of the glycolysis pathway. The partial usage of acetyl-CoA (derived from glucose) for FA synthesis further augments defects in energy substrates for ATP synthesis, as described below. Thus, our data suggest that glucose metabolism is enhanced to compensate for the limited supply of FAs in DKO hearts during fasting by several mechanisms, which include the post-transcriptional and allosteric regulation of the key proteins that regulate glucose uptake and the glycolysis pathway in an insulin-independent manner (Figure VI in the online-only Data Supplement).

The TCA cycle oxidizes acetyl-CoA that is derived from carbohydrates, ketone bodies, fatty acids, and amino acids to produce NADH and reduced form of flavin adenine dinucleotide$_2$ for ATP synthesis in the respiratory chain[24] (Figure VI in the online-only Data Supplement). When acetyl-CoA binds to oxaloacetate, it enters the TCA cycle as citrate. When a surplus of carbohydrates is taken in by an excess diet, however, citrate then serves as the material for FA synthesis instead of ATP synthesis in the TCA cycle (Figure VI in the online-only Data Supplement). We showed that the level of *cis*-aconitate was significantly lower in DKO hearts than in WT during fasting, despite the data that the level of acetyl-CoA was higher in DKO hearts and the level of citrate was comparable between WT and DKO hearts (Figure 5B). In contrast to other components of the TCA cycle whose materials are also supplied by ketone bodies and amino acids (eg, succinate from aceto-acetate, 2-oxoglutarate and succinyl-CoA from amino acids) during fasting, *cis*-aconitate is made only from citrate (derived from acetyl-CoA) and gives rise to only isocitrate. These findings suggest that acetyl-CoA that is derived from glucose is likely to be used for FA synthesis in spite of fasting. In addition to the role of FA as an energy substrate, FAs are also used as essential materials for membrane phospholipids and biologically active compounds such as eicosanoids.[24] Because the FA supply is reduced as a result of disturbance of transendothelial FA transport, FA synthesis is likely to be required via significant glucose uptake in DKO hearts even during fasting to fulfill other demands for FAs. We assume that the deprivation of citrate for FA synthesis could enhance ATP deficiency that may further accelerate glucose uptake and the glycolysis pathway. This scenario can partially account for striking magnitude of glucose uptake relative to reduction of FA uptake in DKO hearts during fasting.

It should be noted that ≈60% of FA uptake remained in DKO heart, indicating that there are FA transport systems that are independent of FABP4/5. As discussed above, capillary endothelial FATP3 and FATP4 are possible candidates that may contribute to the remaining FA uptake in the DKO heart.[3] In addition, vesicular transport, known as transcytosis, is evident in the literature.[25–28] Further studies are required to define the subcellular mechanisms underlying the FA transport via capillary ECs in the heart.

In summary, we demonstrate that FABP4/5 are coexpressed in capillary ECs in heart and skeletal muscle and are required for FA uptake into these tissues. Glucose consumption is dramatically upregulated independently of insulin in the tissues of *fabp4/5* DKO mice to fulfill the energy demand. Our novel findings may have broad and important implications for therapeutic approaches to metabolic disease and heart disease. The targeted inhibition of capillary endothelial FABP4/5 might diminish the uptake of FAs and improve glucose consumption in heart and red skeletal muscles without the need to target metabolic cells or tissues in an insulin-independent manner. Indeed, the orally active small-molecule inhibitor of FABP4, BMS309403, improved several aspects of metabolic syndrome, including type 2

diabetes mellitus and atherosclerosis,[29] which may be attributable, at least in part, to the inhibition of capillary FABP4. Our in vivo demonstration of the regulatory role of FABP4/5 in transendothelial FA transport opens a new research area on the role of this transport system in the treatment and prevention of cardiometabolic disease, such as heart failure associated with metabolic syndrome and type 2 diabetes mellitus.

Materials and Methods

Mice

Mice with a homozygous null mutation in *Fabp4* (*Fabp4*−/−) or *Fabp5* (*Fabp5*−/−) were generated as described previously [1, 2]. Mice that were doubly deficient for *Fabp4* and *Fabp5* (*Fabp4/5* DKO) were generated from an intercross between *Fabp4* (−/−) and *Fabp5* (−/−) mice as described previously[3]. The Institutional Animal Care and Use Committee (Gunma University Graduate School of Medicine) approved all studies.

RNA isolation and Reverse Transcription (RT)–PCR

Total RNA was isolated from various organs using the TRIzol Reagent (Invitrogen). Semi-quantitative RT-PCR was performed with RT-PCR kit (TAKARA, Japan) according to the manufacturer's protocol. Quantitative real-time PCR was performed with SYBR Green PCR Master Mix (Applied Biosystems), according to the manufacturer's instructions. The expression level of the target gene was normalized to the level of GAPDH mRNA. The gene-specific primers for cDNA are listed in supplemental table 1.

Anti-FABP4 Antibody

An anti-FABP4 antibody was affinity-purified from rabbit antisera directed against a GST-tagged human FABP4 (whole molecule) (Shibayagi, Japan). The sensitivity and specificity of this antibody was confirmed by Western blot analysis and immunofluorescence (data not shown).

Immunohistochemical analysis

Organs from mouse and human were fixed with 4% paraformaldehyde and were embedded in paraffin. Immunohistochemistry was performed with antibodies directed against FABP4 (described above), FABP5 (R&D, AF3077) and PECAM/CD31 (R&D, BAF3628) by using the ABC kit (Vector) according to the manufacturer's protocol. Nuclei were stained with hematoxylin. Signals were observed by BIOREVO microscopy (Keyence).

Biodistribution of ^{125}I-BMIPP (15-(p-iodophenyl)-3-(R,S)-methyl pentadecanoic acid) and ^{18}F-FDG (2-fluorodeoxyglucose)

The biodistribution of ^{125}I-BMIPP and ^{18}F-FDG was determined as described previously [4, 5]. Mice received intravenous injections of ^{125}I-BMIPP (5 kBq) and ^{18}F-FDG (100 kBq) via the lateral tail vein in a volume of 100 μl. ^{125}I-BMIPP was a gift from Nihon Medi-Physics Co. Ltd., and ^{18}F-FDG was obtained from batches that were prepared for clinical PET imaging in Gunma University. The animals were sacrificed at 2 hours after injection. The isolated tissues were weighed and counted in a well-type gamma counter (ARC-7001, ALOKA). Each experiment was performed at least twice. PET (Positron Emission Tomography) scan was performed with a small animal PET scanner (Inveon, Siemens) at 2 hours after the intravenous injection of ^{18}F-FDG (10 MBq).

Isolation of cardiac myocytes and ECs from hearts

Primary cultured ventricular myocytes that were isolated from adult mice were prepared as described previously[6]. Collagenase-digested isolated myocytes were incubated in buffer

with increasing concentrations of Ca^{2+}, achieving a final concentration of 1.2 mM Ca^{2+} as in MEM culture media (Sigma Aldrich). Cells were seeded at 30,000 rod-like myocytes/ml on 6-well plates coated with laminin. After a 1 hour incubation in 5% CO_2 at 37°C, the culture media were replaced to remove unattached cells. Three hours later, the uptake of ^{14}C-palmitic acid and ^{3}H-deoxy glucose were carried out as described below.

Uptake of fatty acids and deoxyglucose

For uptake experiments, isolated cardiomyocytes were cultured in MEM medium (Sigma Aldrich) without bovine fetal serum or insulin for three hours. Then, cells were preincubated in glucose-free DMEM (Invitrogen) with or without insulin (1 μM) for twenty minutes. Ten minutes after adding ^{14}C-palmitic acid or ^{3}H-deoxyglucose, cells were washed with ice-cold stop buffer (phosphate buffer saline containing 0.1% bovine serum albumin and 0.2 mM phloretin) and were lysed with lysis buffer (0.1 N NaOH and 0.2% SDS). The radioactivity of the cell lysate was determined by liquid scintillation counter. Experiments were conducted three times.

Measurement of triglyceride in hearts

Hearts were homogenized with buffer containing 50 mM Tris-HCl (pH 7.4), 1% NP40, 0.25% Na-deoxycholate, 150 mM NaCl and 1 mM EDTA. After centrifugation, lipids in the supernatant were extracted with chloroform/methanol (2:1), evaporated and dissolved in isopropanol. Triglyceride contents were determined by Triglyceride E-test Wako (Wako Chemical, Osaka) and were expressed as milligrams of lipid per gram of protein.

Western blot analysis

Western blot analyses were carried out as described previously[7]. Antibodies against insulin receptor β (IRβ, Santa Cruz Biotechnology, sc-711), phosphorylated IR-β (pIRβ, Calbiochem, #407707), AKT (Cell Signaling, #9272), phosphorylated AKT (pAKT, Cell Signaling, #9271), AMP-activated protein kinase (AMPK, Cell Signaling, #2532), phosphorylated AMPK (pAMPK, Cell Signaling, 2531), Glut 4 (R & D, MAB1262), phosphofructokinase 2 (PFK2, Santa Cruz Biotechnology, sc-50956), phosphorylated PFK2 (pPFK2, Santa Cruz Biotechnology, sc-32967), pyruvate dehydrogenase (PDH, MitoScience, MSP07), phosphorylated PDH (pPDH, abcam, ab92696) and α-tubulin (Sigma Aldrich, T6199) were used. Levels of protein expression or phosphorylation were quantified by densitometric analysis with ImageJ software (National Institute of Health).

Metabolome Analysis by CE-MS

Metabolome Analyses were carried out as described previously[8]. Mice were decapitated and ventricles were immediately taken from mice at the age of 3 months after a 24-hour fast. The heart samples were snap-frozen in liquid nitrogen immediately and maintained at −80°C.

Metabolite Extraction—Frozen heart tissue was immediately plunged into methanol (1 ml) that contained internal standards (300 μM each of methionine sulfone for cations and MES for anions) and was homogenized for 1 min to inactivate enzymes. Then, deionized water (500 μl) was added, 300 μl of the solution were transferred to another tube, and 200 μl of chloroform were added, and the mixture was mixed thoroughly. The solution was centrifuged at 12,000 x g for 15 min at 4°C and the 300 μl upper aqueous layer was centrifugally filtered through a Millipore 5-kDa cutoff filter to remove proteins. The filtrate was lyophilized and dissolved in 50 μl of Milli-Q water that contained reference compounds (200 μM each of 3-aminopyrrolidine and trimesate) before CE-MS analysis.

Metabolic Standards—All chemical standards were obtained from common commercial sources and were dissolved in Milli-Q (Millipore) water, 0.1 N HCL or 0.1 N NaOH to obtain 10 mM or 100 mM stock solutions. Working standard mixtures were prepared by diluting stock solutions with Milli-Q water just before injection into the CE-MS. The chemicals used were of analytical or reagent grade.

Instruments—All CE-MS experiments were performed using an Agilent CE Capillary Electrophoresis System that was equipped with an air pressure pump, an Agilent 1100 series MSD mass spectrometer, and an Agilent 1100 series isocratic high performance liquid chromatography pump, a G1603A Agilent CE-MS adapter kit, and a G1607A Agilent CE-MS sprayer kit (Agilent Technologies). System control, data acquisition, and MSD data evaluation were performed using the G2201AA Agilent Chem Station software for CE-MSD.

CE-MS Conditions for Cationic Metabolites—Separations were carried out in a fused silica capillary (50 μm inner diameter x 100 cm total length) that was filled with 1 M formic acid as the electrolyte. Approximately 3 nl of sample solution was injected at 50 mbar for 3 s, and voltage at 30 kV was applied. ESI-MS was conducted in the positive ion mode, and the capillary voltage was set at 4000 V. For MS using the selective ion monitoring mode, deprotonated $[M+H]^+$ ions were monitored for cationic metabolites of interest.

CE-MS Conditions for Anionic Metabolites—A cationic polymer-coated SMILE (+) capillary was obtained from Nacalai Tesque (Kyoto, Japan) and was used as the separation capillary (50 μm inner diameter x 100 cm total length). The electrolyte for the CE separation was 50 mM ammonium acetate solution (pH 8.5). Samples were injected with a pressure injection of 50 mbar for 30 s (30 nl). The applied voltage was set at −30 kV. ESI-MS was conducted in the negative ion mode, and the capillary voltage was set at 3500 V. For MS using the selective ion monitoring mode, deprotonated $[M-H]^-$ ions were monitored for anionic metabolites of interest.

Biochemical measurement

The serum level of glucose was measured by the glutest sensor (Sanwa Kagaku, Aichi, Japan). The serum levels of insulin (Ultrasensitive Mouse Insulin ELISA, Mercodia, Uppsala, Sweden), ketone bodies (CnzyChrom Ketone Body Assay Kit, BioAssay Systems, California), triglycerides (Triglyceride E-test, Wako Chemical, Osaka), non-esterified fatty acids (NEFA C-test, Wako Chemical, Osaka) and total cholesterol (Cholesterol E-test, Wako Chemical, Osaka) were measured according to the manufacturer's protocols.

Statistical Analysis

Statistical analysis was performed in SPSS 20.0. Data are presented as the mean ± SD. Statistical comparisons were performed by using Student's t-test when the experiment included 2 groups. Statistical significance was tested by a 1-way analysis of variance with the Turkey-Kramer post hoc test when experiments included > two groups. The level of significance was set at a probability value of <0.05.

Supplementary Material

Refer to Web version on PubMed Central for supplementary material.

Acknowledgments

We thank Drs Yamada, Kashihara, and Koitabashi for technical advice on the isolation of cardiac myocytes; and Miki Matsui, Yukiyo Tosaka, Keiko Matsukura, and Takako Kobayashi for excellent technical help.

Sources of Funding

This work was supported, in part, by a Grant-in-Aid for Scientific Research from the Japan Society for the Promotion of Science (to M. Kurabayashi and T. Iso), a grant from the Japan Cardiovascular Foundation (to M. Kurabayashi) and grants from the Takeda Science Foundation, Therapeutic Research for Metabolic Syndrome, AstraZeneca, and the Vehicle Racing Commemorative Foundation (to T. Iso). M. Suematsu is supported, in part, by the Japan Science and Technology Agency, Exploratory Research for Advanced Technology, Suematsu Gas Biology Project. G.S. Hotamisligil is supported, in part, by the National Institutes of Health (NIH; DK064360). N.A. Abumrad is supported, in part, by NIH grant DK033301.

Nonstandard Abbreviations and Acronyms

DKO mice	double-knockout mice
EC	endothelial cell
^{18}F-FDG	^{18}F-fluorodeoxyglucose
FA	fatty acid
FABP	fatty acid binding protein
FAT	fatty acid translocase
FATP	FA transport protein
^{125}I-BMIPP	^{125}I-15-(*p*-iodophenyl)-3-(R,S)-methyl pentadecanoic acid
NEFAs	nonesterified fatty acids
PFK	phosphofructokinase
PPARγ	peroxisome proliferator–activated receptor γ
TCA cycle	tricarboxylic acid cycle
TG	triacylglycerol
VEGF	vascular endothelial growth factor
WT	wild type

References

1. van der Vusse GJ. Albumin as fatty acid transporter. Drug Metab Pharmacokinet. 2009; 24:300–307. [PubMed: 19745557]
2. van der Vusse GJ, van Bilsen M, Glatz JF. Cardiac fatty acid uptake and transport in health and disease. Cardiovasc Res. 2000; 45:279–293. [PubMed: 10728348]
3. Hagberg CE, Falkevall A, Wang X, Larsson E, Huusko J, Nilsson I, et al. Vascular endothelial growth factor B controls endothelial fatty acid uptake. Nature. 2010; 464:917–921. [PubMed: 20228789]
4. Goto K, Iso T, Hanaoka H, Yamaguchi A, Suga T, Hattori A, et al. Peroxisome proliferator-activated receptor-? in capillary endothelia promotes fatty acid uptake by heart during long-term fasting. J Am Heart Assoc. 2013; 2:e004861. [PubMed: 23525438]
5. Kanda T, Brown JD, Orasanu G, Vogel S, Gonzalez FJ, Sartoretto J, et al. PPARgamma in the endothelium regulates metabolic responses to high-fat diet in mice. J Clin Invest. 2009; 119:110–124. [PubMed: 19065047]

6. Furuhashi M, Hotamisligil GS. Fatty acid-binding proteins: role in metabolic diseases and potential as drug targets. Nat Rev Drug Discov. 2008; 7:489–503. [PubMed: 18511927]
7. Hotamisligil GS, Johnson RS, Distel RJ, Ellis R, Papaioannou VE, Spiegelman BM. Uncoupling of obesity from insulin resistance through a targeted mutation in aP2, the adipocyte fatty acid binding protein. Science. 1996; 274:1377–1379. [PubMed: 8910278]
8. Maeda K, Uysal KT, Makowski L, Görgün CZ, Atsumi G, Parker RA, et al. Role of the fatty acid binding protein mal1 in obesity and insulin resistance. Diabetes. 2003; 52:300–307. [PubMed: 12540600]
9. Makowski L, Boord JB, Maeda K, Babaev VR, Uysal KT, Morgan MA, et al. Lack of macrophage fatty-acid-binding protein aP2 protects mice deficient in apolipoprotein E against atherosclerosis. Nat Med. 2001; 7:699–705. [PubMed: 11385507]
10. Boord JB, Maeda K, Makowski L, Babaev VR, Fazio S, Linton MF, et al. Combined adipocyte-macrophage fatty acid-binding protein deficiency improves metabolism, atherosclerosis, and survival in apolipoprotein E-deficient mice. Circulation. 2004; 110:1492–1498. [PubMed: 15353487]
11. Maeda K, Cao H, Kono K, Gorgun CZ, Furuhashi M, Uysal KT, et al. Adipocyte/macrophage fatty acid binding proteins control integrated metabolic responses in obesity and diabetes. Cell Metab. 2005; 1:107–119. [PubMed: 16054052]
12. Elmasri H, Karaaslan C, Teper Y, Ghelfi E, Weng M, Ince TA, et al. Fatty acid binding protein 4 is a target of VEGF and a regulator of cell proliferation in endothelial cells. FASEB J. 2009; 23:3865–3873. [PubMed: 19625659]
13. Masouyé I, Hagens G, Van Kuppevelt TH, Madsen P, Saurat JH, Veerkamp JH, et al. Endothelial cells of the human microvasculature express epidermal fatty acid-binding protein. Circ Res. 1997; 81:297–303. [PubMed: 9285630]
14. Opie, LH. Heart Physiology. Baltimore, MD: Lippincott Williams & Wilkins; 2004. p. 306-354.
15. de Lange P, Moreno M, Silvestri E, Lombardi A, Goglia F, Lanni A. Fuel economy in food-deprived skeletal muscle: signaling pathways and regulatory mechanisms. FASEB J. 2007; 21:3431–3441. [PubMed: 17595346]
16. Steinberg GR, Kemp BE. AMPK in Health and Disease. Physiol Rev. 2009; 89:1025–1078. [PubMed: 19584320]
17. Furuhashi M, Fucho R, Görgün CZ, Tuncman G, Cao H, Hotamisligil GS. Adipocyte/macrophage fatty acid-binding proteins contribute to metabolic deterioration through actions in both macrophages and adipocytes in mice. J Clin Invest. 2008; 118:2640–2650. [PubMed: 18551191]
18. Cao H, Gerhold K, Mayers JR, Wiest MM, Watkins SM, Hotamisligil GS. Identification of a lipokine, a lipid hormone linking adipose tissue to systemic metabolism. Cell. 2008; 134:933–944. [PubMed: 18805087]
19. Luptak I, Balschi JA, Xing Y, Leone TC, Kelly DP, Tian R. Decreased contractile and metabolic reserve in peroxisome proliferator-activated receptor-alpha-null hearts can be rescued by increasing glucose transport and utilization. Circulation. 2005; 112:2339–2346. [PubMed: 16203912]
20. Hajri T, Han XX, Bonen A, Abumrad NA. Defective fatty acid uptake modulates insulin responsiveness and metabolic responses to diet in CD36-null mice. J Clin Invest. 2002; 109:1381–1389. [PubMed: 12021254]
21. Schaap FG, Binas B, Danneberg H, van der Vusse GJ, Glatz JF. Impaired long-chain fatty acid utilization by cardiac myocytes isolated from mice lacking the heart-type fatty acid binding protein gene. Circ Res. 1999; 85:329–337. [PubMed: 10455061]
22. Binas B, Danneberg H, McWhir J, Mullins L, Clark AJ. Requirement for the heart-type fatty acid binding protein in cardiac fatty acid utilization. FASEB J. 1999; 13:805–812. [PubMed: 10224224]
23. Augustus AS, Buchanan J, Park TS, Hirata K, Noh HL, Sun J, et al. Loss of lipoprotein lipase-derived fatty acids leads to increased cardiac glucose metabolism and heart dysfunction. J Biol Chem. 2006; 281:8716–8723. [PubMed: 16410253]
24. Marray, RK. Harper's Illustrated Biochemistry. New York, NY: McGraw Hill Professional; 2009.
25. Fawcett, DW. A Textbook of Histology. New York, NY: Chapman & Hall; 1994. p. 368-409.

26. Bartelt A, Bruns OT, Reimer R, Hohenberg H, Ittrich H, Peldschus K, et al. Brown adipose tissue activity controls triglyceride clearance. Nat Med. 2011; 17:200–205. [PubMed: 21258337]

27. Bharadwaj KG, Hiyama Y, Hu Y, Huggins LA, Ramakrishnan R, Abumrad NA, et al. Chylomicron- and VLDL-derived lipids enter the heart through different pathways: *in vivo* evidence for receptor- and non-receptor-mediated fatty acid uptake. J Biol Chem. 2010; 285:37976–37986. [PubMed: 20852327]

28. Fielding CJ. Metabolism of cholesterol-rich chylomicroms. Mechanism of binding and uptake of cholesteryl esters by the vascular bed of the perfused rat heart. J Clin Invest. 1978; 62:141–151. [PubMed: 659628]

29. Furuhashi M, Tuncman G, Görgün CZ, Makowski L, Atsumi G, Vaillancourt E, et al. Treatment of diabetes and atherosclerosis by inhibiting fatty-acid-binding protein aP2. Nature. 2007; 447:959–965. [PubMed: 17554340]

References

1. Hotamisligil GS, Johnson RS, Distel RJ, Ellis R, Papaioannou VE, Spiegelman BM. Uncoupling of obesity from insulin resistance through a targeted mutation in ap2, the adipocyte fatty acid binding protein. Science. 1996; 274:1377–1379. [PubMed: 8910278]

2. Maeda K, Uysal KT, Makowski L, Gorgun CZ, Atsumi G, Parker RA, Bruning J, Hertzel AV, Bernlohr DA, Hotamisligil GS. Role of the fatty acid binding protein mal1 in obesity and insulin resistance. Diabetes. 2003; 52:300–307. [PubMed: 12540600]

3. Maeda K, Cao H, Kono K, Gorgun CZ, Furuhashi M, Uysal KT, Cao Q, Atsumi G, Malone H, Krishnan B, Minokoshi Y, Kahn BB, Parker RA, Hotamisligil GS. Adipocyte/macrophage fatty acid binding proteins control integrated metabolic responses in obesity and diabetes. Cell Metab. 2005; 1:107–119. [PubMed: 16054052]

4. Coburn CT, Knapp FF Jr, Febbraio M, Beets AL, Silverstein RL, Abumrad NA. Defective uptake and utilization of long chain fatty acids in muscle and adipose tissues of cd36 knockout mice. J Biol Chem. 2000; 275:32523–32529. [PubMed: 10913136]

5. Hajri T, Han XX, Bonen A, Abumrad NA. Defective fatty acid uptake modulates insulin responsiveness and metabolic responses to diet in cd36-null mice. J Clin Invest. 2002; 109:1381–1389. [PubMed: 12021254]

6. Koitabashi N, Danner T, Zaiman AL, Pinto YM, Rowell J, Mankowski J, Zhang D, Nakamura T, Takimoto E, Kass DA. Pivotal role of cardiomyocyte tgf-beta signaling in the murine pathological response to sustained pressure overload. J Clin Invest. 121:2301–2312. [PubMed: 21537080]

7. Shimizu T, Tanaka T, Iso T, Matsui H, Ooyama Y, Kawai-Kowase K, Arai M, Kurabayashi M. Notch signaling pathway enhances bone morphogenetic protein 2 (bmp2) responsiveness of msx2 gene to induce osteogenic differentiation and mineralization of vascular smooth muscle cells. J Biol Chem. 2011; 286:19138–19148. [PubMed: 21471203]

8. Endo J, Sano M, Katayama T, Hishiki T, Shinmura K, Morizane S, Matsuhashi T, Katsumata Y, Zhang Y, Ito H, Nagahata Y, Marchitti S, Nishimaki K, Wolf AM, Nakanishi H, Hattori F, Vasiliou V, Adachi T, Ohsawa I, Taguchi R, Hirabayashi Y, Ohta S, Suematsu M, Ogawa S, Fukuda K. Metabolic remodeling induced by mitochondrial aldehyde stress stimulates tolerance to oxidative stress in the heart. Circ Res. 2009; 105:1118–1127. [PubMed: 19815821]

Significance

Fatty acid binding protein 4/5 (FABP4/5), which are coexpressed in capillary endothelial cells in heart and skeletal muscle, are required for FA uptake into these tissues. Glucose consumption is dramatically upregulated independently of insulin in the tissues of fabp4/5 double-knockout mice to compensate for restricted FA usage. Our novel findings may have broad and important implications for therapeutic approaches to metabolic and heart diseases. The targeted inhibition of capillary endothelial Fatty acid binding protein 4/5 might diminish the uptake of FAs and improve glucose consumption in the heart and red skeletal muscles without the need to target metabolic cells or tissues in an insulin-independent manner. Our in vivo demonstration of the regulatory role of fatty acid binding protein 4/5 in transendothelial FA transport opens a new research area on the role of this transport system in the treatment and prevention of cardiometabolic disease, such as heart failure associated with metabolic syndrome and type 2 diabetes mellitus.

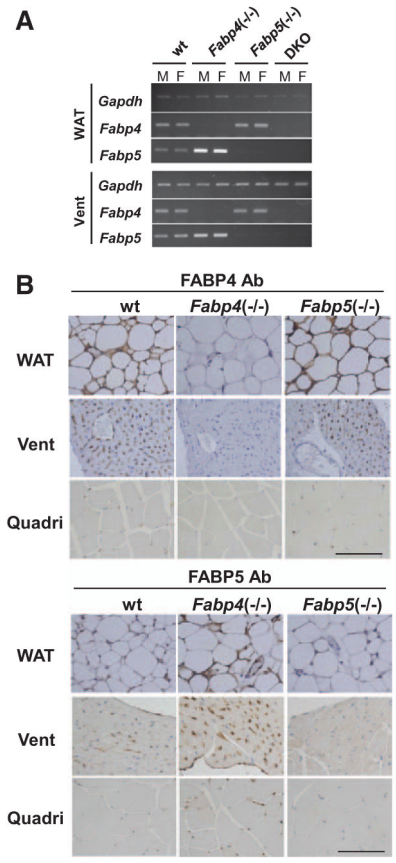

Figure 1.

Fatty acid binding protein 4 (FABP4) and FABP5 are expressed in capillary endothelial cells. **A**, Expression of mRNA for *Fabp4/5* in white adipose tissue (WAT) and ventricles (Vent) from wild-type (WT), *Fabp4*$^{-/-}$, *Fabp5*$^{-/-}$, and *Fabp4/5* double-knockout (DKO) mice. Total RNA was isolated for semiquantitative reverse transcription polymerase chain reaction. **B**, Immunohistochemical localization of FABP4/5 was detected with antibodies (Ab) directed against FABP4 and FABP5 in indicated tissues from wild-type (WT), *Fabp4*$^{-/-}$, and *Fabp5*$^{-/-}$ mice. Nuclei were stained with hematoxylin. Scale bar, 100 μm. See also Figure I in the online-only Data Supplement. F indicates female; M, male; and Quadri, quadriceps.

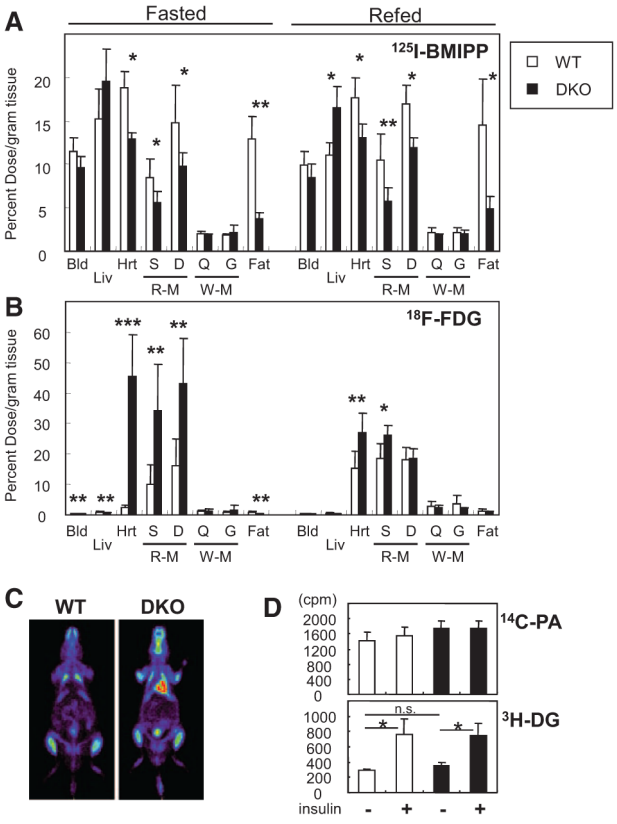

Figure 2.

Glucose is a major energy substrate in the hearts and red skeletal muscles of fatty acid binding protein 4/5 (*Fabp4/5*) double-knockout (DKO) mice even during fasting. **A** and **B**, After a 24-hour fast, mice received intravenous injection of ^{125}I-15-(*p*-iodophenyl)-3-(R,S)-methyl pentadecanoic acid (^{125}I-BMIPP; 5 kBq) and ^{18}F-fluorodeoxyglucose (^{18}F-FDG; 100 kBq) via the lateral tail vein. The animals were euthanized at 2 hours after injection. The uptake of ^{125}I-BMIPP (**A**) and ^{18}F-FDG (**B**) by indicated organs from wild-type (WT) or *Fabp4/5* DKO male mice was counted in a well-type gamma counter with or without 2-hour refeeding (n=6; **P*<0.05). **C**, Representative positron emission tomography image of ^{18}F-FDG 2 hours after injection in WT and *Fabp4/5* DKO mice after a 24-hour fast. **D**, Baseline and insulin-stimulated uptake of FAs and glucose in isolated cardiac myocytes from WT and *Fabp4/5* DKO mice. The uptake of ^{14}C-palmitic acid (^{14}C-PA) and ^{3}H-deoxyglucose (^{3}H-DG) were measured (n=6) in the presence or absence of insulin (1 mmol/L). **P*<0.05. See also Figure II in the online-only Data Supplement. Bld indicates blood; D, diaphragma, Fat, gonadal fat pad; G, gastrocnemius; Hrt, heart; Liv, liver; Q, quadriceps; R-M, red skeletal muscle (soleus); S, soleus; and W-M, white skeletal muscle (quadriceps).

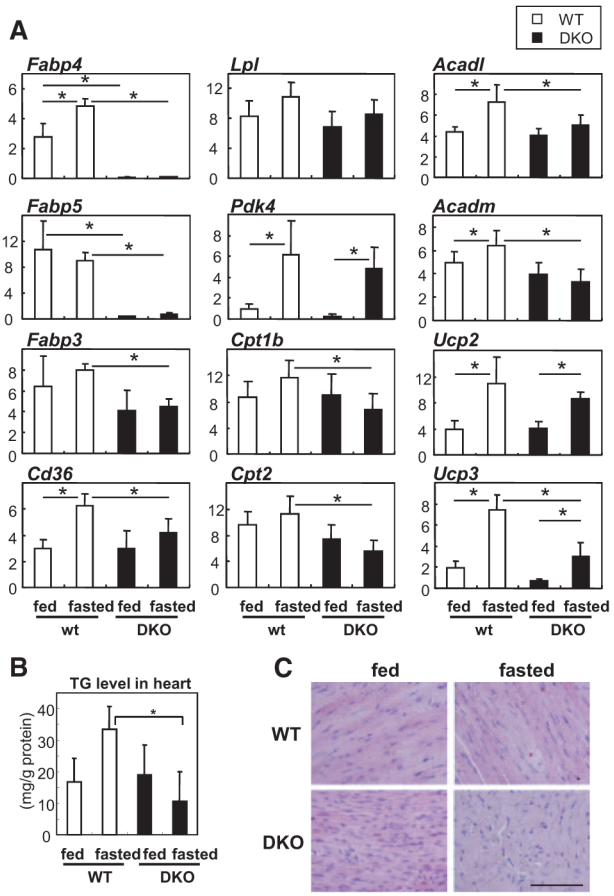

Figure 3.

Expression of genes associated with fatty acid (FA) metabolism in hearts. **A**, Relative mRNA expression of genes associated with FA metabolism in the hearts of wild-type (WT) and fatty acid binding protein 4/5 (*Fabp4/5*) double-knockout (DKO) mice with or without a 24-hour fast. The level of each transcript is determined by real-time polymerase chain reaction (n=6). Data are shown as the mean±SD. **P*<0.05. **B**, Triacylglycerol (TG) content in the hearts of WT and *Fabp4/5* DKO mice with or without a 24-hour fast (n=5; **P*<0.05). **C**, TG droplet is detected by oil red O stain in the hearts of WT and DKO mice with or without fasting. Scale bar, 100 μm.

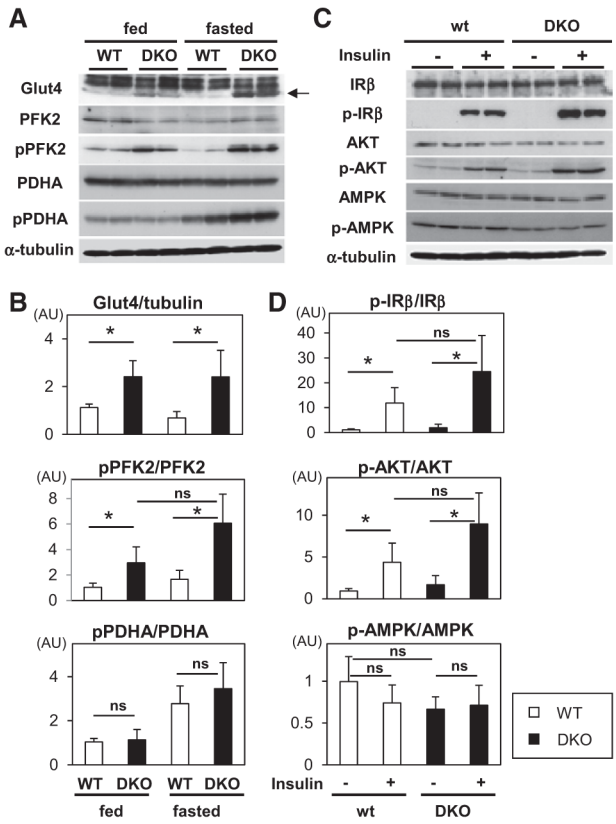

Figure 4.

Glucose uptake is accelerated independently of insulin signaling during fasting. **A**, Protein expression and phosphorylation were determined by Western blot analysis in the hearts before and after a 24-hour fast. **B**, Levels of protein expression or phosphorylation were quantified by densitometric analysis (n=6). Data are shown as the mean±SD. **P*<0.05. **C**, Insulin (5 U/kg) was injected into the peritoneal cavity after a 24-hour fast. Twenty minutes later, protein was extracted from isolated hearts for Western blot analysis. **D**, Levels of phosphorylation were quantified by densitometric analysis (n=6). AMPK indicates AMP-activated protein kinase; AU, arbitrary unit; IRβ, insulin receptor-β; p-AMPK, phosphorylated AMPK; PFK2, phosphofructokinase-2; PDHA, pyruvate dehydrogenase-α; p-IR, phosphorylated IR; and pPFK, phophorylated PFK.

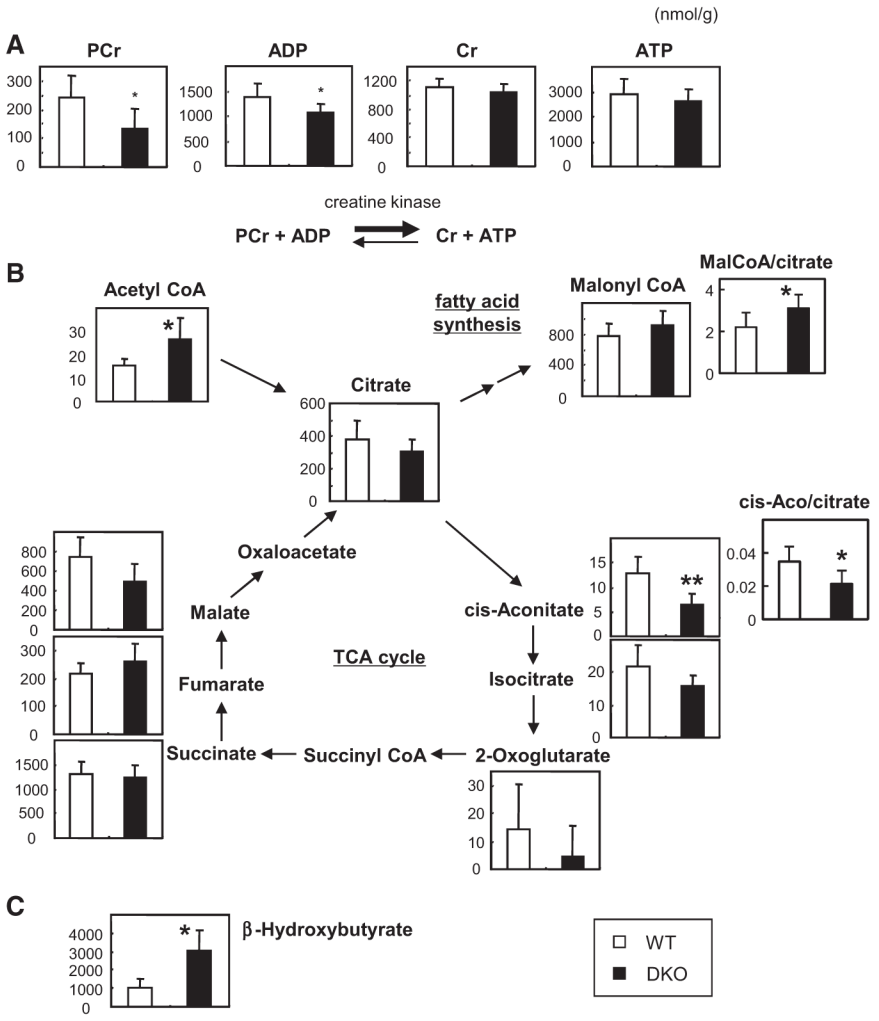

Figure 5.

Metabolome analyses of fatty acid binding protein *4/5* (*Fabp4/5*) double-knockout (DKO) hearts. Indicated metabolites from the hearts of wild-type (WT) and *Fabp4/5* DKO mice after a 24-hour fast were measured by capillary electrophoresis-mass spectrometry (n=6). **P*<0.05, ***P*<0.01. **A**, Energy reserve (phosphocreatine [PCr] plus ADP) was decreased in *Fabp4/5* DKO hearts. **B**, Metabolites in the tricarboxylic acid (TCA) cycle and malonyl-CoA as an intermediate of FA synthesis. **C**, The level of β-hydroxybutyrate was markedly higher in DKO hearts.

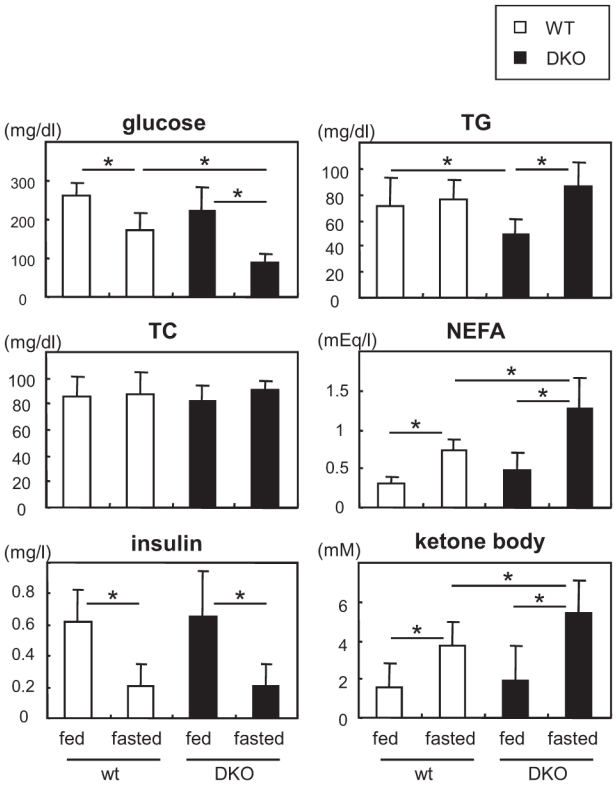

Figure 6.

Serum levels of nonesterified fatty acids (NEFAs) and ketone bodies are higher in fatty acid binding protein 4/5 (*Fabp4/5*) double-knockout (DKO) mice after a 24-hour fast. Serum levels of indicated biochemical parameters were measured before and after a 24-hour fast (n=8). **P*<0.05. TC indicates total cholesterol; and TG, triacylglycerol.